Hindawi Publishing Corporation
Journal of Nanotechnology
Volume 2014, Article ID 653198, 9 pages
http://dx.doi.org/10.1155/2014/653198

Research Article

Controlled Synthesis of Gold Nanoparticles Using *Aspergillus terreus* IF0 and Its Antibacterial Potential against Gram Negative Pathogenic Bacteria

Eepsita Priyadarshini,[1] Nilotpala Pradhan,[1,2] Lala B. Sukla,[2] and Prasanna K. Panda[2]

[1] *Academy of Scientific and Innovative Research, CSIR-Institute of Minerals and Materials Technology, Bhubaneswar 751013, India*
[2] *Bioresources Engineering Department, CSIR-Institute of Minerals and Materials Technology, Bhubaneswar 751013, India*

Correspondence should be addressed to Nilotpala Pradhan; nilotpala_pradhan@yahoo.co.in

Received 18 February 2014; Revised 30 April 2014; Accepted 30 April 2014; Published 29 May 2014

Academic Editor: Paresh Chandra Ray

Biosynthesis of monodispersed nanoparticles, along with determination of potential responsible biomolecules, is the major bottleneck in the area of bionanotechnology research. The present study focuses on an ecofriendly, ambient temperature protocol for size controlled synthesis of gold nanoparticles, using the fungus *Aspergillus terreus* IF0. Gold nanoparticles were formed immediately, with the addition of chloroauric acid to the aqueous fungal extract. Synthesized nanoparticles were characterized by UV-Vis spectroscopy, TEM-EDX, and XRD analysis. Particle diameter and dispersity of nanoparticles were controlled by varying the pH of the fungal extract. At pH 10, the average size of the synthesized particles was in the range of 10–19 nm. Dialysis to obtain high and low molecular weight fraction followed by FTIR analysis revealed that biomolecules larger than 12 kDa and having –CH, –NH, and –SH functional groups were responsible for bioreduction and stabilization. In addition, the synthesized gold nanoparticles were found to be selectively bactericidal against the pathogenic gram negative bacteria, *Escherichia coli*.

1. Introduction

Metal nanoparticles have been gaining importance in the past years because of their unique properties. Substantial research has been directed towards their reliable synthesis to explore their potential applications [1, 2]. Amongst the noble metals (silver, gold, and platinum), gold nanoparticles (GNPs) are of increasing interest due to their use in divergent fields of science [3–5]. The distinct optical property of GNPs makes them quite useful in the field of biomedicine. GNPs are being extensively used for colorimetric detection of DNA and proteins, in form of biosensors, bioimaging, diagnostics, and therapeutic agents [6–9].

Over the years, several physicochemical methods have been used for GNP synthesis [10–13]. However, these synthetic protocols not only are hazardous and energy consuming, but also pose a major disadvantage of adsorption of toxic chemical species onto the surface of nanoparticles making them unsuitable for biomedical applications [14]. Hence, researchers are focused towards synthesis of biocompatible nanoparticles leading to the development of a biological route for nanoparticle synthesis. Biological approach towards nanoparticle synthesis involves the use of an environmentally acceptable solvent system along with nontoxic reducing and capping agents [15]. A number of biological agents like bacteria, algae, fungus, and plant extracts have been employed for biogenic nanoparticle synthesis [16–19]. Among the reported microorganisms, fungus offers the advantage of easy handling and fast downstream processing and allows feasible large scale synthesis of nanoparticles due to the high secretion of enzymes and proteins [20]. Cytosolic extracts of the fungi *Candida albicans*, *Aspergillus niger*, *Penicillium* sp., and *Aspergillus clavatus* have been successfully used for GNP synthesis [21–24]. However, with reference to the ongoing researches in fungal nanobiotechnology, most of the work converges at the preliminary steps of synthesis. Identification of the variables involved, along with elucidation of the responsible biomolecules, can greatly assist in achieving

controlled synthesis of nanoparticles. Compared to other metal nanoparticles, GNP offers the advantage of being stable and nontoxic and allows easy surface modification potential. Hence, synthesis of monodispersed GNPs can make them suitable agents for clinical and pharmaceutical applications.

The present work aimed at developing a feasible, single-step, and ecofriendly approach towards size regulated synthesis of biogenic GNPs, using the fungus *Aspergillus terreus* IF0. The extracellular culture filtrate (ECF) of the fungus served as the reaction medium for GNP biosynthesis. To the best of our knowledge, this is the first report of such rapid synthesis of GNP employing a microbial strain. The main objective of the present study was to control the size and dispersity of biosynthesized GNPs, by modulating the initial pH of the ECF. Furthermore, the probable mechanism behind the functionality of pH on size controlled biosynthesis of GNP is proposed. The synthesized nanoparticles were characterized by UV-Vis spectroscopy, transmission electron microscopy (TEM), X-ray diffraction (XRD), and Fourier transform infrared spectroscopy (FTIR). In addition, the antibacterial potential of the synthesized GNPs was determined against pathogenic gram positive and negative bacteria.

2. Materials and Method

2.1. Organisms and Growth Conditions. The fungus used in the present study was selected from among the various laboratory stock cultures (CSIR-IMMT, Bhubaneswar). Pure culture of the fungal strain was maintained on Potato Dextrose Agar (PDA, Himedia) slants. Morphological characterization of the strain was done using optical microscopy by lactophenol cotton blue staining. For experimental purpose, the fungal culture was grown in a cost effective mineral salt medium (MSM) comprised of (gL^{-1}) KH_2P0_4 (0.5), K_2HPO_4 (1.5), NaCl (0.5), $MgSO_4$ (0.3), NH_4Cl (3), and sucrose (20). The initial pH of media was adjusted to 6.8. Fungal spores were aseptically inoculated in sterile growth media and incubated in a shaker incubator (Kuhner) at 35°C and 150 rpm for 72 h. Fungal biomass obtained was filtered and washed thoroughly with sterile distilled water to remove media components. The washed biomass was again resuspended in 100 mL of sterile distilled water for another 72 h under similar conditions. The biomass was finally removed by filtration and the extracellular filtrate (ECF) obtained was used for subsequent experiments. Resuspension of the biomass in distilled water subjects it to a stress condition and assists in the release of extracellular enzymes and metabolites.

2.2. Gold Nanoparticle Biosynthesis and Deciphering the Responsible Biomolecules. The potential of the fungal extract to biosynthesize GNP was studied, by adding chloroauric acid, $HAuCl_4$ (Sigma Aldrich) to ECF. For all the experiments, $HAuCl_4$ was used at a final concentration of 1 mM. Control experiment without the addition of $HAuCl_4$ was also run under similar conditions. The initial pH of fungal ECF was varied to understand the effect of pH on size and shape distribution of GNPs. pH of ECF was varied by use of dilute NaOH and HCl.

With an objective to divulge the biomolecules responsible for GNP biosynthesis, dialysis of the fungal ECF was carried out using dialysis membrane tubing having a molecular weight cut-off of 12 kDa. The biomolecules (proteins and metabolites) present in the ECF were separated based on their molecular weights by dialyzing it against sterile distilled water for 24 h. The extracts were labelled as EI (extract present inside the dialysis tubing) and EO (extract present outside dialysis tubing), respectively. EI was mainly composed of high molecular weight proteins and other soluble components of ECF retained inside the tubing whereas EO was composed of low molecular weight proteins and other soluble components of ECF diffusing out of the tubing. Both the extracts (EI and EO) were thereafter examined for GNP biosynthesis.

2.3. Characterization of Biosynthesized Nanoparticles. The capability of the fungus to reduce gold ions to form GNPs was observed by the visible change in colour from light yellow to the characteristic colour of GNPs. GNP biosynthesis was monitored using a UV-Vis spectroscopy (CECIL) in the range of 200–900 nm at regular time intervals. Size and shape of the synthesized GNP were determined using transmission electron microscopy (TEM) by drop-coating the sample onto a carbon coated copper grid and drying under an IR lamp. The instrument used for analysis was a FEI, TECNAI-G2, and 20-TWIN electron microscope operating at 200 kV equipped with a GATAN CCD camera along with an energy dispersive X-ray spectrophotometer (EDS). Crystalline nature of synthesized nanoparticles was characterized using XRD. XRD analysis was carried out on Philips X'pert Pro, Panalytical, X-ray powder diffractometer having Cu-K_α ($\lambda = 1.54$ Å) radiation working at 40 kV/30 mA. The X-ray patterns were obtained in the 2θ range of 10–79°. Sample for XRD analysis was prepared by coating a thin film of the colloidal GNP solution onto a glass substrate. To examine the potential functional groups involved in biosynthesis, FTIR analysis was carried out using FTIR-Perkin-Elmer (Model Spectrum 1) in the range of 4000–400 cm^{-1} at a resolution of 2 cm^{-1}. Few drops of the sample were layered on a circular glass slide and allowed to dry resulting in formation of a thin film which was subsequently analyzed.

2.4. Determination of Antibacterial Activity of Biosynthesized Nanoparticles. The antibacterial activity of biosynthesized GNP was determined against the pathogenic gram negative (*Escherichia coli*—ATCC 35218) and gram positive (*Streptococcus mutans*—MTCC 497) bacteria. In addition, tests were also carried out against some other gram positive bacteria (*Bacillus stearothermophilus*—ATCC-7953; *Rhodococcus erythropolis*—MTCC-3951*; Rhodococcus rhodochrous*—MTCC-3552). Antibacterial activity was determined using the conventional well diffusion method. Wells of 6 mm diameter were dug on nutrient agar plates and overnight grown bacterial cultures were spread uniformly on the plates using sterile cotton swabs. 80 μL of biosynthesized GNP and fungal ECF (negative control) was loaded into the individual wells. All the plates were incubated overnight in an incubator maintained at 37°C. After the incubation period, the plates were observed

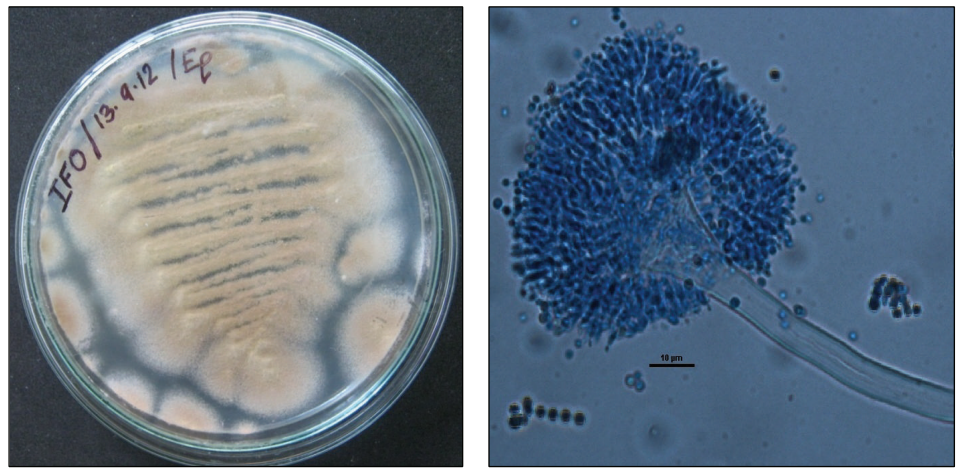

Figure 1: Morphological features of the fungus: (a) growth on PDA plate, (b) phase contrast microscopic image.

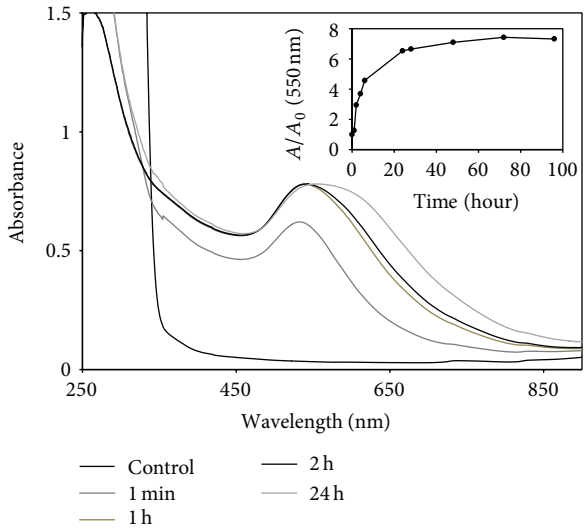

Figure 2: UV-Vis spectra of gold nanoparticles synthesized at different time intervals. Inset shows the absorbance intensity of gold nanoparticles with progressing time (A and A_0 are absorbance at respective time and ECF only, respectively).

for formation of inhibition zone around the well, which represents antibacterial activity. The zone of inhibition was determined by measuring the diameter of the clear inhibition zone formed around the well.

3. Result and Discussion

3.1. Synthesis of Gold Nanoparticles and Their Characterisation. The fungal strain used in the present study was screened for GNP biosynthesis and identified using taxonomic keys with microscopic observations. The fungal spores were sand brown in colour (Figure 1(a)). Colony morphology and phase contrast microscopic image (Figure 1(b)) characterized the fungus as *Aspergillus terreus* IF0 [25].

With the addition of $HAuCl_4$ to the fungal ECF, immediate (within few seconds) change in colour from light yellow to purple was observed. Further confirmation of GNP synthesis was carried out by UV-visible spectral analysis which revealed the appearance of a sharp peak at 550 nm. The observed purple colour and the absorption peak in the range of 500–600 nm are characteristic features of GNP and are termed as surface plasmon resonance (SPR) [26]. Figure 2 presents the UV-Vis spectra of GNP synthesized at different time intervals. A sharp and narrow SPR peak was observed at 550 nm within few seconds of treating $HAuCl_4$ with ECF. With progressing reaction time the absorption intensity of SPR peak was found to increase along with red shift and peak broadening. This signifies polydispersity and increase in the size of synthesized GNP with progressing reaction time. Absorbance intensity was found to increase sharply and almost reached saturation after 72 h of treatment (inset in Figure 2), suggesting the completion of reduction reaction. The study thus infers that the fungal extract was quite efficient in rapid reduction of gold ions to form GNPs. Earlier studies have revealed that microorganisms such as bacteria [27] and fungus [18, 22] were capable of reducing gold ions to GNP, whereas the time required for the bioreduction process ranged from 24 to 48 h. This is a major drawback of biosynthetic procedures compared to chemical methods. Hence, the potential of this fungus towards such rapid GNP synthesis within a narrow size range presents a significant advancement in the area of biological nanoparticle synthesis.

3.2. Effect of pH Modulation on Gold Nanoparticle Biosynthesis. In the present study, the biomolecules secreted by the fungal strain reduce Au^{3+} to form Au nanoparticles. Though the scenario behind formation of biogenic GNP has not yet been clearly understood, undoubtedly it involves a reduction reaction, involving the transfer of electrons and protons. Hence, variation of pH could play a significant role in biosynthesis of GNPs. Prior literature reveals that pH is a major factor in controlling size and monodispersity of nanoparticles [28, 29]; still the exact

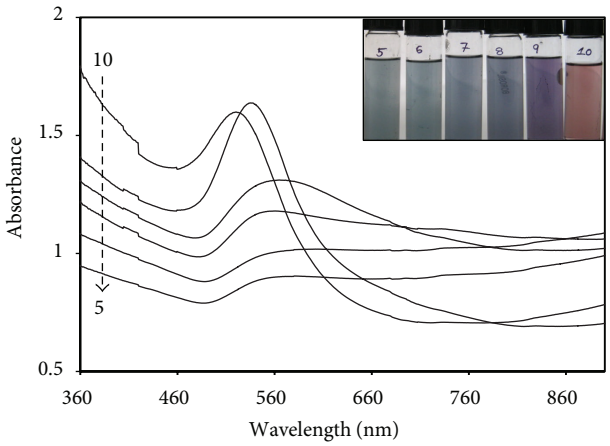

Figure 3: UV-Vis spectra depicting the effect of initial pH of ECF on GNP synthesis after 24 hours of reaction.

reaction mechanism is not clearly understood. To determine the effect of pH on nanoparticle formation, size, and dispersity, initial pH of ECF was varied from 5 to 10 using dilute HCl/NaOH, keeping all other parameters the same.

Figure 3 presents the UV-Vis spectra obtained for GNP synthesized at different pH of ECF. As already mentioned, at the inherent pH (pH 8) of ECF, a SPR peak was obtained at 550 nm. TEM micrographs of the synthesized GNPs confirmed the particles to be in nanorange. The nanoparticles synthesized at the inherent pH were basically polydispersed, varying in shape from spherical to rod as evident from TEM analysis (Figure 4(b)). Histogram of particle size distribution showed that the synthesized particles were mainly 20–29 nm in size (Figure 5(b)). When pH of ECF gradually increased from 5 to 10, narrowing of peaks along with blue shift was observed. At pH 5 the SPR peak was positioned at 565 nm whereas it shifted to 520 nm at pH 10 (Figure 3). Blue shift indicates decrease in the size of synthesized GNP. At pH 5, 6, and 7 broad SPR peaks were obtained, which can be ascribed to the polydispersity of synthesized nanoparticles [29]. TEM micrographs shown in Figure 4(a) represent GNP synthesized at pH 5. Basically, elongated, triangular, and rod shaped nanoparticles were observed, illustrating a wide distribution in shape of synthesized nanoparticles. However, at alkaline pH of 9 and 10 intense and sharp SPR peaks were observed. Narrowing of SPR peaks signifies monodispersity of particles which was in well agreement with TEM analysis. Figure 4(c) presents the TEM image of GNP synthesized at pH 10. At pH 10, the particles were of 10–19 nm size range as revealed from size distribution histogram (Figure 5(c)). Size distribution histogram shown in Figure 5 revealed that the synthesized GNPs show a decrease in size with increasing pH. The results thus suggest that with gradually increasing pH there is an increase in reduction rate with controlled nucleation and capping that favours the synthesis of GNPs of reduced size. Thus, by modulating the pH of the fungal ECF towards alkalinity, we were able to considerably limit the size and shape of GNP.

EDX profile shown in Figure 6(a) features strong Au signals from synthesized GNPs. The carbon and oxygen peak can be ascribed to the biomolecules present in the ECF and Cu peaks are due to the copper grids used in TEM analysis. The corresponding SAED image (Figure 6(b)) shows several diffraction ring patterns, depicting the different phase arrangement and crystalline nature of synthesized GNP. The crystalline elemental nature of GNP was further confirmed from XRD spectra. Figure 6(c) represents the XRD pattern of GNP synthesized using the fungal extract. It shows peaks in the 2θ range 10°–79° which corresponds well to the crystal facets of (111), (200), and (220) of gold which matched the standard XRD data (JCPDS Card Number 00-001-1172).

3.3. Partial Identification of Biomolecules Responsible for Gold Nanoparticle Synthesis. Studies mentioned above evidently indicate the involvement of biomolecules in fungal extract for the bioreduction of gold ions to form GNP. Conformation of the presence and involvement of protein molecules was brought about from protein assay studies. To further elucidate the possible biomolecules involved in bioreduction, dialysis of the ECF was carried out. Higher protein concentration was observed in the EI fraction compared to EO as evident from the UV absorbance at 280 nm (Figure 7) and proteins estimation by Folin-Lowry method [30]. The UV-Vis spectra presented in Figure 7 show distinct SPR peak characteristics of GNP in case of EI, which was basically composed of high molecular weight proteins (greater than 12 kDa) and other soluble components of ECF. However, the absence of SPR peak in EO (composed of low molecular weight proteins and other soluble components) specifies its inability in bioreduction of gold ions. This confirms that large molecular weight proteins are mainly responsible for the formation of GNPs.

Further, FTIR analysis enabled the identification of potential functional groups involved in bioreduction and subsequent capping of GNP. FTIR spectra of the fungal extract (ECF) and synthesized GNP are shown in Figure 8. It indicates the disappearance as well as appearance of new peaks after synthesis of nanoparticles. FTIR spectra showed a broad contour in the range of 3600–3220 cm^{-1}, which indicates the presence of –OH groups. The peak positioned at 2730 cm^{-1} could be attributed to the –CH stretch of aldehydes. The disappearance of this peak signifies their active participation in reduction of gold ions. After GNP synthesis, appearance of peaks at 1255 cm^{-1} and 1117 cm^{-1} is attributed to the C-N stretch of aliphatic amine [31]. FTIR spectra show disappearance of peaks at 812 cm^{-1} and 577 cm^{-1} attributed to bending vibration of –CH and –NH groups of amines. Similarly disappearance of peak at 683 cm^{-1} is due to disulphides group indicating its involvement in GNP formation [31]. Complete absence of these bands after reduction signifies that amino acids such as cysteine and methionine may be involved in the reduction and/or stabilization process. The involvement of these functional groups strongly suggests

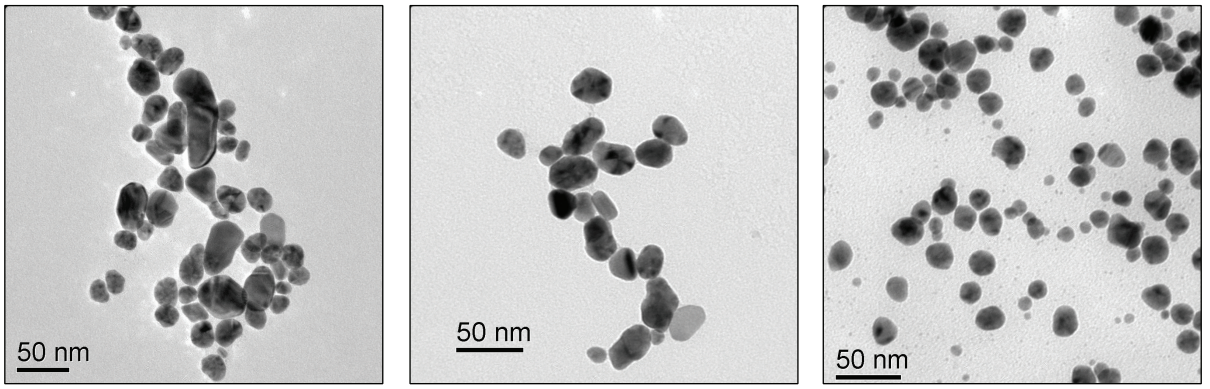

Figure 4: TEM micrographs of synthesized GNP at different pH of ECF: (a) pH 5, (b) pH 8 (inherent pH), and (c) pH 10.

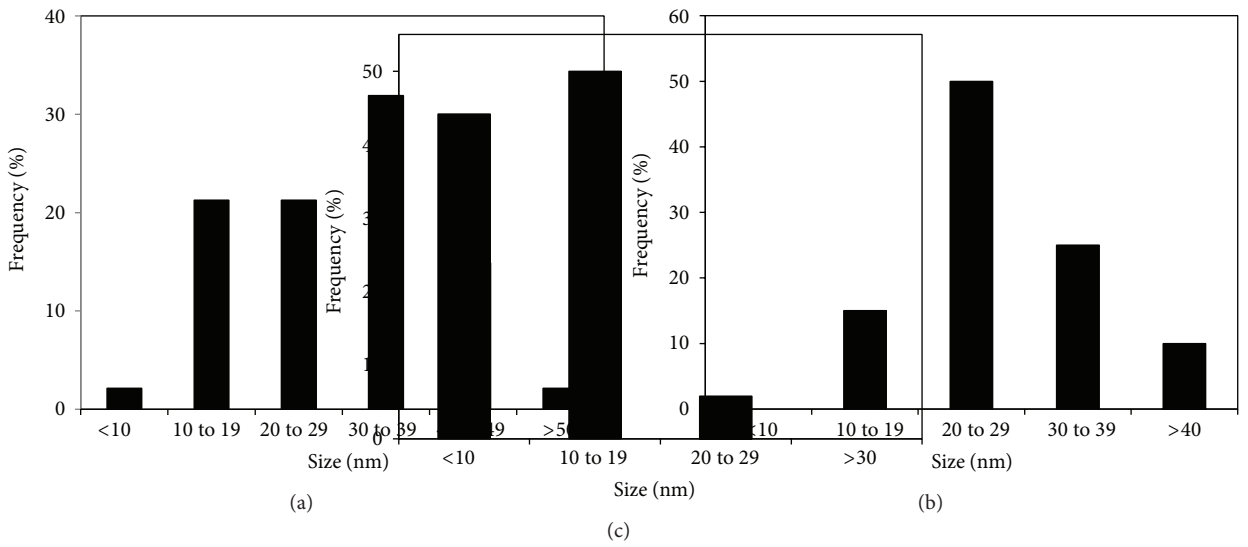

Figure 5: Particle size histogram of GNPs synthesized at different pH of ECF: (a) pH 5, (b) pH 8 (inherent pH), and (c) pH 10.

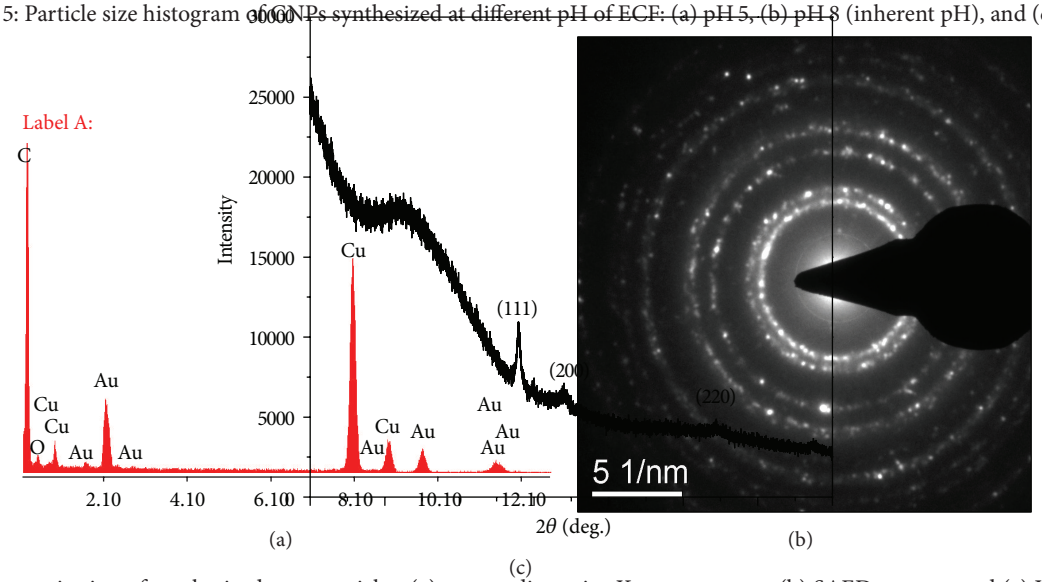

Figure 6: Characterisation of synthesized nanoparticles: (a) energy dispersive X-ray spectrum, (b) SAED pattern, and (c) XRD analysis of the synthesized GNP.

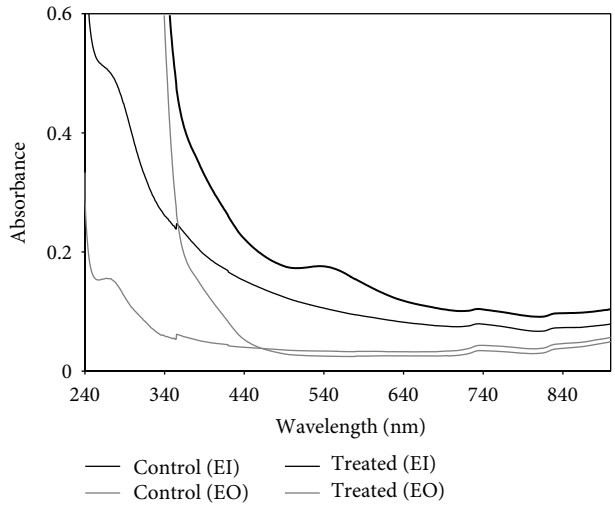

Figure 7: UV-Vis spectra showing GNP biosynthesis in the dialyzed ECF extracts.

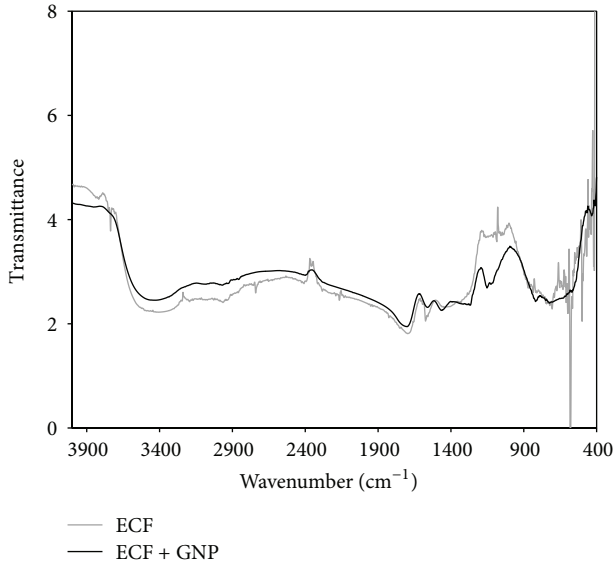

Figure 8: FTIR spectra of fungal extract (ECF) and synthesized GNP.

the role of protein molecules in the bioreductive synthesis of GNP.

3.4. Antibacterial Activity of Biosynthesized Gold Nanoparticles. Toxicity of nanoparticles against pathogenic microorganisms has made them evolve as potential agents in clinical applications. Considering the fact that GNPs are relatively stable and nontoxic, we explored the antibacterial activity of the synthesized GNPs against gram positive and gram negative bacteria. Fungal ECF (negative control) did not show antibacterial activity against any of the bacterial cultures. However, biosynthesized GNP showed a distinct inhibition zone of 1.3 cm against the gram negative bacteria *E. coli* (Figure 9(a)), but it was not effective against the gram positive bacteria *S. mutans* (Figure 9(b)). Antibacterial test against other gram positive bacteria (*B. stearothermophilus*, *R. erythropolis*, and *R. rhodochrous*) also showed a negative result. The result thus indicates that the biosynthesized GNP was toxic to tested gram negative bacteria only and not to the tested gram positive bacterial strains. Literature studies have revealed that GNPs inhibit bacterial growth by generating holes in the cell wall, resulting in release of cell contents, or they bind with the DNA inhibiting its uncoiling thereby transcription [32]. However, in the present case the probable reason behind the selective antibacterial activity might be the external structural differences between gram positive and negative bacteria. However, the exact reason behind the antibacterial activity of biosynthesized GNP needs to be fully understood. Since gram negative bacteria are less susceptible to antibiotics compared to gram positive bacteria, GNP synthesized using this fungal culture can provide an effective means towards selectively inhibiting the disease causing gram negative bacterial strains.

3.5. Proposed Mechanism behind Controlled GNP Synthesis. Bioreduction is the primary mechanism behind the synthesis of metal nanoparticles. Microbial bioreduction basically involves the use of biomolecules as proteins and carbohydrates [33, 34]. Reduction of metal ions in such an environment is the result of electron transfer from proteins to metal ions. Formation of nanoparticle nucleation point and subsequent growth is perceived to be dependent on the initial pH of the fungal extract. Size of resulting nanoparticles was greatly controlled by increasing the pH of fungal extract.

In view of the present study, FTIR data (Figure 8) enumerated the involvement of –CH, –NH, and –SH functional groups in the reduction process. It is thereby speculated that amino acids such as cysteine and methionine may be responsible for GNP biosynthesis. The fungal biomolecules reduce $AuCl4^-$ leading to the formation of GNPs. At an acidic pH, the electrostatic interaction between these reducing agents and $AuCl4^-$ is quite high, which results in a decrease in the reduction reaction. Growth rate of nanoparticles thereby predominates over nucleation rate resulting in the formation of heterogenous and large sized nanoparticles. With increasing pH there is predominance of OH^- ions that offers high electrostatic repulsion that prevents aggregation of particles. The greater colloidal stability obtainable at high pH results in synthesis of nanoparticles of a diminishing size [35]. Figure 10 illustrates the proposed mechanism behind GNP biosynthesis at different pH of fungal ECF.

Researchers are currently focused on physicochemical synthesis of monodispersed nanoparticles. However, our study provides a single-step approach towards controlling the size of GNPs in an ecofriendly approach by feasible modulation of pH of the fungal ECF. Thus, this simple method of biogenic nanoparticle synthesis with uniform size and properties can provide significant applications in the field of biomedicines.

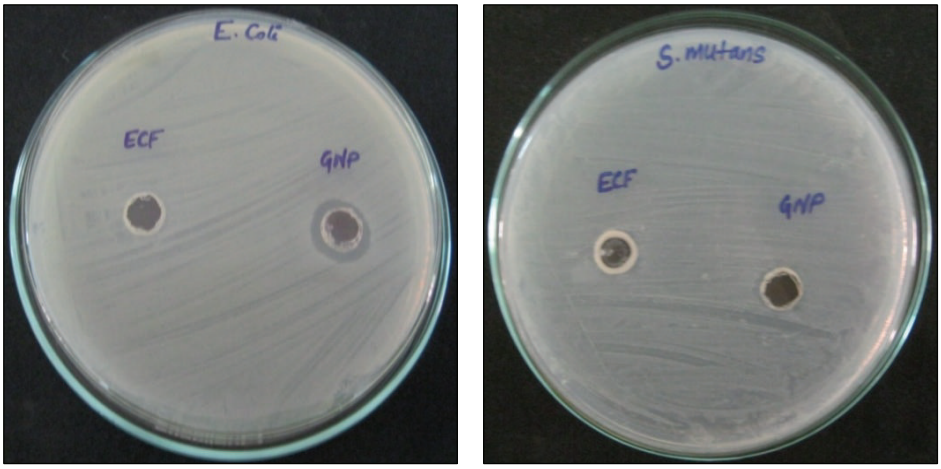

Figure 9: Antibacterial activity of fungal ECF and biosynthesized GNP against different bacterial cultures: (a) *Escherichia coli*, (b) *Streptococcus mutans*.

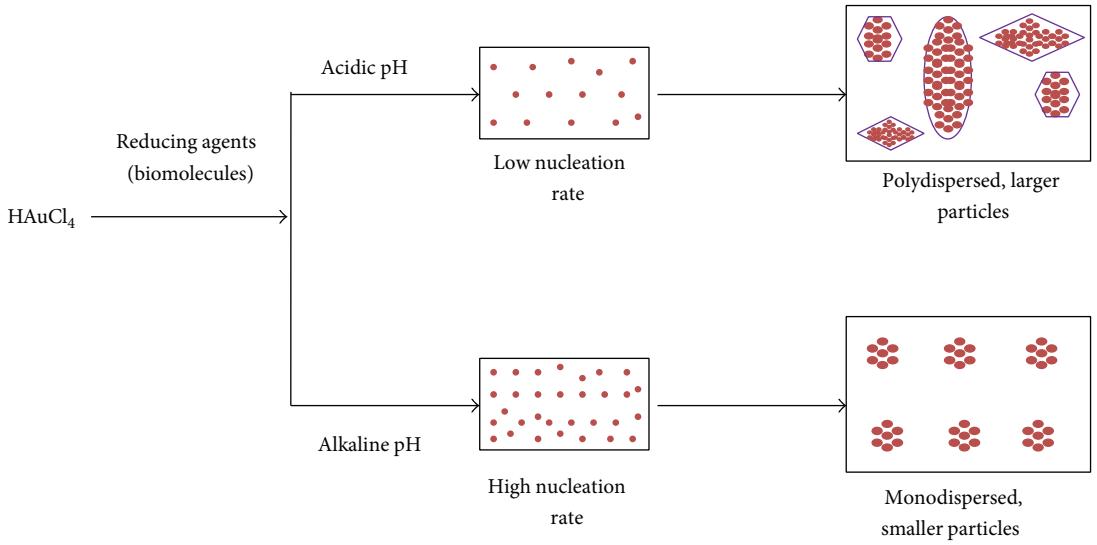

Figure 10: Proposed scheme of GNP synthesis at different pH of fungal extract.

4. Conclusion

A single-step cost effective and ecofriendly biogenic protocol for synthesizing GNP using fungal extract is hereby reported. GNP synthesis occurred within few seconds of adding gold salt to the extract, thus confirming bioreduction. Modulation of initial pH of the fungal extract resulted in a significant variation in size and dispersity of synthesized nanoparticles. Alkaline pH of 10 favoured the synthesis of nanoparticles in the size range of 10–19 nm. It was revealed that protein molecules greater than 12 kDa and having –CH, –NH, and –SH functional groups were basically responsible for bioreduction. The biosynthesized GNP showed antibacterial activity against pathogenic gram negative bacteria, *Escherichia coli*. The one-step biogenic method provides a rapid route for the controlled synthesis of GNP and thus offers better alternative to the energy consuming physicochemical synthetic procedures. Additionally, the antibacterial property of synthesized GNP holds promise in clinical applications and towards the selective killing of pathogenic gram negative strains in a green ecofriendly approach. The study thus imparts a feasible approach towards size controlled synthesis of GNPs for clinical and medical applications.

Conflict of Interests

The authors declare that there is no conflict of interests regarding the publication of this paper.

Acknowledgments

The first author would like to express her sincere thanks to the Department of Science and Technology, India, for fellowship under Inspire Scheme. TEM, XRD, and FTIR analysis were

carried out by Mr. Ajit Dash and Mrs. Swagatika Mohanty to whom the authors' sincere thanks are due.

References

[1] P. K. Jain, X. Huang, I. H. El-Sayed, and M. A. El-Sayed, "Noble metals on the nanoscale: optical and photothermal properties and some applications in imaging, sensing, biology, and medicine," *Accounts of Chemical Research*, vol. 41, no. 12, pp. 1578–1586, 2008.

[2] M. A. El-Sayed, "Some interesting properties of metals confined in time and nanometer space of different shapes," *Accounts of Chemical Research*, vol. 34, no. 4, pp. 257–264, 2001.

[3] Y. H. Ngo, D. Li, G. P. Simon, and G. Garnier, "Gold nanoparticle-paper as a three-dimensional surface enhanced raman scattering substrate," *Langmuir*, vol. 28, no. 23, pp. 8782–8790, 2012.

[4] N. R. Tiwari, A. Rathore, A. Prabhune, and S. K. Kulkarni, "Gold nanoparticles for colorimetric detection of hydrolysis of antibiotics by penicillin G acylase," *Advances in Bioscience and Biotechnology*, vol. 1, pp. 322–329, 2010.

[5] A. Gangula, R. Podila, M. Ramakrishna, L. Karanam, C. Janardhana, and A. M. Rao, "Catalytic reduction of 4-nitrophenol using biogenic gold and silver nanoparticles derived from breynia rhamnoides," *Langmuir*, vol. 27, no. 24, pp. 15268–15274, 2011.

[6] X. L. Luo, J. J. Xu, Y. Du, and H. Y. Chen, "A glucose biosensor based on chitosan-glucose oxidase-gold nanoparticles biocomposite formed by one-step electrodeposition," *Analytical Biochemistry*, vol. 334, no. 2, pp. 284–289, 2004.

[7] Y. C. Cao, R. Jin, and C. A. Mirkin, "Nanoparticles with Raman spectroscopic fingerprints for DNA and RNA detection," *Science*, vol. 297, no. 5586, pp. 1536–1540, 2002.

[8] X. Shi, S. Wang, S. Meshinchi et al., "Dendrimer-entrapped gold nanoparticles as a platform for cancer-cell targeting and imaging," *Small*, vol. 3, no. 7, pp. 1245–1252, 2007.

[9] S. Boca, D. Rugina, A. Pintea, L. Barbu-Tudoran, and S. Astilean, "Flower-shaped gold nanoparticles: synthesis, characterization and their application as SERS-active tags inside living cells," *Nanotechnology*, vol. 22, no. 5, Article ID 055702, 2011.

[10] D. Riabinina, J. Zhang, M. Chaker, J. Margot, and D. Ma, "Size control of gold nanoparticles synthesized by laser ablation in liquid media," *ISRN Nanotehnology*, vol. 2012, Article ID 2978635, 5 pages, 2012.

[11] S. Dong and S. Zhou, "Photochemical synthesis of colloidal gold nanoparticles," *Materials Science and Engineering B: Solid-State Materials for Advanced Technology*, vol. 140, no. 3, pp. 153–159, 2007.

[12] S. Hsu and I. J. B. Lin, "Synthesis of gold nanosheets through thermolysis of mixtures of long chain 1-Alkylimidazole and hydrogen tetrachloroaurate(III)," *Journal of the Chinese Chemical Society*, vol. 56, no. 1, pp. 98–106, 2009.

[13] W. Liu, X. Yang, and L. Xie, "Size-controlled gold nanocolloids on polymer microsphere-stabilizer via interaction between functional groups and gold nanocolloids," *Journal of Colloid and Interface Science*, vol. 313, no. 2, pp. 494–502, 2007.

[14] V. Parashar, R. Parashar, B. Sharma, and A. C. Pandey, "Parthenium leaf extract mediated synthesis of silver nanoparticles: a novel approach towards weed utilization," *Digest Journal of Nanomaterials and Biostructures*, vol. 4, no. 1, pp. 45–50, 2009.

[15] J. Xie, J. Y. Lee, D. I. C. Wang, and Y. P. Ting, "Silver nanoplates: from biological to biomimetic synthesis," *ACS Nano*, vol. 1, no. 5, pp. 429–439, 2007.

[16] B. M. M. Ganesh and P. Gunasekaran, "Production and structural characterization of crystalline silver nanoparticles from *Bacillus cereus* isolate," *Colloids and Surfaces B: Biointerfaces*, vol. 74, no. 1, pp. 191–195, 2009.

[17] A. Schrofel, G. Kratosova, M. Bohunicka, E. Dobrocka, and I. Vavra, "Biosynthesis of gold nanoparticles using diatoms—silica-gold and EPS-gold bionanocomposite formation," *Journal of Nanoparticle Research*, vol. 13, no. 8, pp. 3207–3216, 2011.

[18] E. Priyadarshini, N. Pradhan, L. B. Sukla, P. K. Panda, and B. K. Mishra, "Biogenic synthesis of floral-shaped gold nanoparticles using a novel strain, *Talaromyces flavus*," *Annals of Microbiology*, 2013.

[19] M. O. Montes, A. Mayoral, F. L. Deepak et al., "Anisotropic gold nanoparticles and gold plates biosynthesis using alfalfa extracts," *Journal of Nanoparticle Research*, vol. 13, no. 8, pp. 3113–3121, 2011.

[20] P. Mukherjee, A. Ahmad, D. Mandal et al., "Bioreduction of $AuCl_4^-$ Ions by the Fungus, *Verticillium sp.* and surface trapping of the gold nanoparticles formed," *Angewandte Chemie International Edition*, vol. 40, no. 19, pp. 3585–3588, 2001.

[21] A. Chauhan, S. Zubair, S. Tufail et al., "Fungus-mediated biological synthesis of gold nanoparticles: potential in detection of liver cancer," *International Journal of Nanomedicine*, vol. 6, pp. 2305–2319, 2011.

[22] N. Soni and S. Prakash, "Synthesis of gold nanoparticles by the fungus *Aspergillus niger* and its efficacy against mosquito larvae," *Reports in Parasitology*, vol. 2012, article 2, 7 pages, 2012.

[23] L. Du, L. Xian, and J. Feng, "Rapid extra-/intracellular biosynthesis of gold nanoparticles by the fungus *Penicillium* sp," *Journal of Nanoparticle Research*, vol. 13, no. 3, pp. 921–930, 2011.

[24] V. C. Verma, R. N. Kharwar, S. K. Singh, R. Solanki, and S. Prakash, "Correction to biofabrication of anisotropic gold nanotriangles using extract of endophytic *Aspergillus clavatus* as a dual functional reductant and stabilizer," *Nanoscale Research Letters*, vol. 6, article 261, 16 pages, 2011.

[25] D. Ellis, S. Davis, H. Alexiou, R. Handke, and R. Bartley, *Descriptions of Medical Fungi*, Adelaide Medical Centre for Women and Children, Adelaide, Austraila, 2nd edition, 2007.

[26] P. Mulvaney, "Surface plasmon spectroscopy of nanosized metal particles," *Langmuir*, vol. 12, no. 3, pp. 788–800, 1996.

[27] S. K. Srivastava, R. Yamada, C. Ogino, and A. Kondo, "Biogenic synthesis and characterization of gold nanoparticles by *Escherichia coli* K12 and its heterogeneous catalysis in degradation of 4-nitrophenol," *Nanoscale Research Letters*, vol. 8, article 70, 9 pages, 2013.

[28] R. R. Nayak, N. Pradhan, D. Behera et al., "Green synthesis of silver nanoparticle by *Penicillium purpurogenum* NPMF: the process and optimization," *Journal of Nanoparticle Research*, vol. 13, no. 8, pp. 3129–3137, 2011.

[29] J. Nam, N. Won, H. Jin, H. Chung, and S. Kim, "pH-induced aggregation of gold nanoparticles for photothermal cancer therapy," *Journal of the American Chemical Society*, vol. 131, no. 38, pp. 13639–13645, 2009.

[30] O. H. Lowry, N. J. Rosenbrough, A. L. Farr, and R. J. Randall, "Protein measurement with the Folin phenol reagent," *The Journal of Biological Chemistry*, vol. 193, no. 1, pp. 265–275, 1951.

[31] R. M. Silverstin and F. X. Webster, *Spectrometric Identification of Organic Compounds*, University of Michigan, Ann Arbor, Mich, USA; Wiley, New York, NY, USA, 6th edition, 1998.

[32] A. Rai, A. Prabhune, and C. C. Perry, "Antibiotic mediated synthesis of gold nanoparticles with potent antimicrobial activity and their application in antimicrobial coatings," *Journal of Materials Chemistry*, vol. 20, no. 32, pp. 6789–6798, 2010.

[33] K. M. Moghaddam, "An introduction to microbial metal nanoparticle preparation method," *Journal of Young Investigators*, vol. 19, article 23, 2010.

[34] K. B. Narayan and N. Shaktivel, "Biological synthesis of metal nanoparticles by microbes," *Advances in Colloid and Interface Science*, vol. 156, no. 1-2, pp. 1–13, 2010.

[35] X. Shi, K. Sun, and J. R. Baker Jr., "Functionalized, dendrimer-stabilized gold nanoparticles," *Journal of Physical Chemistry C: Nanomaterials and Interfaces*, vol. 112, no. 22, pp. 8251–8258, 2009.